

Original article

Calcareous nannofossil biostratigraphy of the Thomel Level (OAE2) in the Lambruisse section, Vocontian Basin, southeast France[☆]

Biostratigraphie à nannofossiles calcaires du Niveau Thomel (OAE2) dans la coupe de Lambruisse, Bassin Vocontien, Sud-Est de la France

Allan Gil S. Fernando^{a,*}, Reishi Takashima^b, Hiroshi Nishi^c, Fabienne Giraud^d, Hisatake Okada^{c,e}

^a National Institute of Geological Sciences, College of Science, University of the Philippines, Diliman, Quezon City 1101, Philippines

^b Creative Research Initiative Sousei L-Station, Hokkaido University, N-21, W-10, Kita-ku, Sapporo 001-0021, Japan

^c Division of Earth and Planetary Sciences, Graduate School of Science, Hokkaido University, N-10, W-8, Kita-ku, Sapporo 060-0810, Japan

^d UMR-CNRS 5125 « Paléoenvironnements et Paléobiosphère », campus de la Doua, université Lyon 1, rue Raphaël-Dubois, 69622 Villeurbanne cedex, France

^e Office of the Vice President, Hokkaido University, N-8, W-5, Kita-ku, Sapporo 060-0808, Japan

Received 1 December 2008; accepted 15 November 2009

Available online 3 December 2009

Abstract

The Thomel Level of the Lambruisse section in the Vocontian Basin (southeast France), which is marked by intercalations of black shales and organic-rich marls, accumulated during the oceanic anoxic event 2 (OAE2) occurring in the Cenomanian-Turonian (C-T) boundary interval. Calcareous nannofossil biostratigraphic investigation of this interval revealed a total of five nannofossil zones, corresponding to the UC3-UC8 zones (Middle Cenomanian-Middle Turonian) as defined by Burnett. Biostratigraphically important taxa observed in the section include *Cretarhabdus striatus*, *Axopodorhabdus albianus*, *Lithraphidites acutus*, *Corollithion kennedyi*, *Helenea chiastia*, *Quadrum gartneri*, *Q. intermedium*, *Eiffellithus eximius*, *Eprolithus octopetalus* and *E. eptapetalus*. The two nannofossil events commonly used in the delineation of the C-T boundary, namely the LO of *H. chiastia* and the FO of *Q. gartneri*, occur less than 2 m apart in the studied section. These two bioevents define the limits of the UC6 nannofossil Zone and occur within the *Whiteinella archaeocretacea* foraminifer Zone. Previous litho- and chemostratigraphic analyses indicate that the $\delta^{13}\text{C}$ profile of the section corresponds well with changes in lithofacies and fluctuations in the total organic carbon (TOC) and calcium carbonate content of the section. Initial increase in the $\delta^{13}\text{C}$ values occurs within the UC3-UC4a undifferentiated zone, coinciding with the onset of the deposition of the organic-rich sediments of the Thomel Level and a drastic decline in the CaCO_3 values. The plateau of high $\delta^{13}\text{C}$ values, on the other hand, occurs within the UC5 zone, between the LO of *C. kennedyi* and the LO of *H. chiastia* (and FO of *Q. gartneri*). This interval of high $\delta^{13}\text{C}$ values also corresponds to the interval of high TOC and low CaCO_3 values. The integrated nannofossil, planktonic foraminifer and $\delta^{13}\text{C}$ data provide a precise biostratigraphic and chemostratigraphic framework of the C-T boundary in the Lambruisse section that can be used in future studies in the Vocontian Basin and allow correlations with other well-studied C-T boundary sections.

© 2009 Elsevier Masson SAS. All rights reserved.

Keywords: Calcareous nannofossils; Biostratigraphy; Cenomanian-Turonian boundary; Oceanic anoxic event 2 (OAE2); Vocontian Basin; Southeast France

Résumé

Le Niveau Thomel de la coupe de Lambruisse dans le Bassin Vocontien (SE France), caractérisé par des intercalations de black shales et de marnes riches en matière organique, s'est déposé durant l'événement océanique anoxique (OAE) 2, à la limite Cénomanién-Turonien. L'étude biostratigraphique des nannofossiles calcaires de cet intervalle a permis la reconnaissance de 5 zones de nannofossiles, correspondant aux zones UC3-UC8 (Cénomanién moyen-Turonien moyen) définies par Burnett. Les taxons importants pour la biostratigraphie et reconnus dans la coupe sont : *Cretarhabdus striatus*, *Axopodorhabdus albianus*, *Lithraphidites acutus*, *Corollithion kennedyi*, *Helenea chiastia*, *Quadrum gartneri*, *Q. intermedium*, *Eiffellithus eximius*, *Eprolithus octopetalus* et *E. eptapetalus*. Les deux bio-événements généralement utilisés pour définir la

[☆] Corresponding editor: Emanuela Mattioli.

* Corresponding author.

E-mail addresses: afernando@nigs.upd.edu.ph, agsfernando@yahoo.com (A.G.S. Fernando).

limite Cénomaniens-Turonien, correspondant à la dernière occurrence (LO) de *H. chiastia* et à la première occurrence (FO) de *Q. gartneri*, sont séparés de moins de 2 m dans la coupe étudiée. Ces deux bio-événements définissent les limites de la zone de nannofossile UC6 et sont reconnus dans la zone de foraminifère planctonique à *Whiteinella archaeoeretacea*. Des analyses litho- et chimostratigraphiques réalisées sur cette coupe dans une étude précédente, montrent que les variations observées du $\delta^{13}\text{C}$ correspondent aux changements du lithofaciès et des teneurs en carbone organique (COT) et carbonate de calcium. L'augmentation initiale des valeurs du $\delta^{13}\text{C}$ est reconnue dans les zones de nannofossiles calcaires UC3-UC4a, coïncidant avec les premiers dépôts de sédiments riches en matière organique du Niveau Thomel, et avec une chute drastique de la teneur en carbonate de calcium. Puis les valeurs élevées du $\delta^{13}\text{C}$ forment un plateau, daté de la zone de nannofossile UC5, et situé entre les dernières occurrences de *C. kenedyi* et de *H. chiastia* (et la première occurrence de *Q. gartneri*). Ce plateau correspond également à un intervalle où le COT est élevé et les teneurs en CaCO_3 faibles. Les données intégrées : nannofossiles calcaires, foraminifères planctoniques et $\delta^{13}\text{C}$, fournissent un cadre biostratigraphique et chimostratigraphique précis de la limite C-T dans la coupe de Lambruisse, pouvant être réutilisé dans les études futures du Bassin Vocontien, et permettant des corrélations avec les autres coupes bien étudiées de la limite C-T.

© 2009 Elsevier Masson SAS. Tous droits réservés.

Mots clés : Nannofossiles calcaires ; Biostratigraphie ; Limite Cénomaniens-Turonien ; Événement océanique anoxique 2 (OAE2) ; Bassin Vocontien ; Sud-Est de la France

1. Introduction

The Oceanic Anoxic Event encompassing the Cenomanian-Turonian (C-T) boundary interval, called OAE2, is considered the type example of the Mesozoic OAEs (Schlanger and Jenkyns, 1976; Kolonic et al., 2005). The event was associated with a large and abrupt perturbation in atmospheric $p\text{CO}_2$ (Kuypers et al., 1999), changes/turnover in the marine macro- and microfauna (Erbacher et al., 1996; Premoli Silva et al., 1999; Gale et al., 2000; Leckie et al., 2002; Erba, 2004), changes in ocean water chemistry (Kuypers et al., 2002; Snow et al., 2005), and a pronounced positive excursion in the $\delta^{13}\text{C}$ record of the marine carbonate and marine and terrestrial organic matter (Scholle and Arthur, 1980; Pratt and Threlkeld, 1984; Jarvis et al., 1988; Gale et al., 1993; Jenkyns et al., 1994; Hasegawa, 1997; Tsikos et al., 2004). The positive shift in the $\delta^{13}\text{C}$ curve has been hypothesized as related to the widespread burial of isotopically light (^{12}C -enriched) organic matter, in response to enhanced oceanic productivity due to injection of biolimiting metals into the surface waters during the formation of the Caribbean Plateau large igneous province (LIP) and increased submarine volcanism, ocean crust production and hydrothermal activity (Schlanger and Jenkyns, 1976; Duncan and Bralower, 2002; Leckie et al., 2002; Erba, 2004). Basalts from the Caribbean Plateau LIP were previously determined to have radiometric ages of about 88–91 Ma (Turonian-Coniacian interval; Sinton and Duncan, 1997; Shipboard Scientific Party, 2000). Recent studies, however, suggest a slightly older age of 92–95 Ma, within the C-T interval (Duncan and Bralower, 2002). This new radiometric age confirms the presence and the possible contribution of a major submarine volcanism in the deposition of the OAE2 black shales. This assumption is further substantiated by a drop in the strontium isotope ($^{87}\text{Sr}/^{86}\text{Sr}$) and trace metal distribution data across the C-T boundary due to increased rates of ocean crust production and elevated submarine volcanism (Bralower et al., 1997; Leckie et al., 2002; Snow et al., 2005). Similar to the Early Aptian OAE1a, OAE2 is also considered as a high productivity oceanic anoxic event (P-OAE; Erbacher et al., 1996).

Since the pioneer work of Schlanger and Jenkyns (1976), several studies have already been done with respect to the impact of OAEs on the evolution and distribution of marine organisms. A number of these investigations concentrated on the carbonaceous sediments from the C-T boundary interval, resulting in a comprehensive global picture of the event (Erbacher et al., 1999). Calcareous nannofossils and other microfossils (i.e., radiolaria, benthic and planktonic foraminifers) experienced a high rate of turnover within this interval as a result of the rapid sequence of extinction of several taxa prior and during the main period of the OAE2 anoxia (Premoli Silva et al., 1999; Leckie et al., 2002; Erba, 2004). Changes in calcareous nannofossil assemblages across the C-T boundary have already been documented in the Western Interior Basin (Bralower, 1988), and in several localities of the Boreal, Tethyan and Atlantic Regions: Northern Europe and Southern England (Bralower, 1988; Jarvis et al., 1988; Paul et al., 1999; Gale et al., 2000); Spain (Lamolda et al., 1997); Italy (Luciani and Cobianchi, 1999; Premoli Silva et al., 1999; Erba, 2004); Jordan (Schulze et al., 2004); North Africa (Bralower, 1988; Bauer et al., 2001); and the equatorial Atlantic (Hardas and Mutterlose, 2006, 2007).

Black shales of local to regional importance crop out in the Vocontian Basin in southeast France. Although a number of calcareous nannofossil studies have already been done in the area, most focused on older black shale deposits (e.g., Herrle, 2003; Giraud et al., 2003; Herrle and Mutterlose, 2003; Herrle et al., 2003; Reboulet et al., 2003, 2005; Bornemann et al., 2005; Heimhofer et al., 2006; Duchamp-Alphonse et al., 2007). Studies regarding OAE2 black shales in France are limited to planktonic foraminifers and ammonite biostratigraphy, geochemical and carbon isotope analyses (e.g., Crumière, 1990; Crumière et al., 1990; Thomel, 1991; Grosheny and Tronchetti, 1993; Grosheny et al., 2006).

The present study reports on the nannofossil assemblages, their distribution and biostratigraphy, along with TOC, carbonate and $\delta^{13}\text{C}$ data across the C-T boundary interval of the Lambruisse section. The present study, in addition, aims to provide a refined, integrated biostratigraphic and chemostratigraphic framework for better constraining this boundary in the Vocontian Basin.

2. Geology of the study area and lithology

The Lambruisse section is located in the southeastern part of the Vocontian Basin, which forms a part of the hemipelagic intrashelf basin of the European Tethyan passive margin (Crumière et al., 1990; Wilpshaar et al., 1997; Fig. 1). Major tectonic changes occurred in this basin at the beginning of the Late Cretaceous, with transition from dominant extensional regime until the Albian, to dominant compression and transpression from the Cenomanian (e.g., Joseph et al., 1989; Fries and Parize, 2003). During the mid-Cretaceous, the Vocontian Basin was estimated to be located between paleolatitudes 25°–30°N (Savostin et al., 1986; Hay et al., 1999; Bornemann et al., 2005), within the Tethyan paleobiogeographic nannofloral province of Burnett et al. (1998). Paleobathymetry estimates for the Vocontian Basin are still under debate. Based on the dinoflagellate studies of Wilpshaar and Leereveld (1994), the basin was estimated to have paleodepths of a few hundred meters, which is in great contrast to the 1000 to 2000 m paleodepth estimated by Cotillon and Rio (1984). A more recent study on benthic foraminifers in the basin by Holbourn et al. (2001) suggested a paleodepth of 1000 m, which is comparable to the estimated values of Cotillon and Rio (1984).

The Lambruisse section is located in the eastern part of the Vocontian Basin, south of Ondres (Fig. 1). In this part of the Vocontian Basin, the Cenomanian hemipelagic sediments consist of alternating limestone-marl bundles separated by large marly intervals (Crumière, 1990; Wilpshaar et al., 1997; Herrle, 2002; Bornemann et al., 2005). Across the C-T boundary interval, the alternations consist of several black shale layers (Grosheny et al., 2006). Called the Thome Level (e.g., Crumière, 1990), the distinct dark-gray marl and black shale interval are the regional expression of the OAE2 in southeastern France.

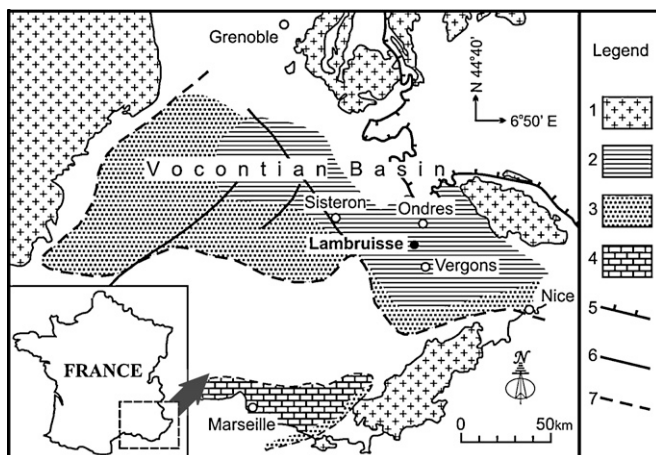


Fig. 1. Geologic map of the study area and location of the Lambruisse section in the Vocontian Basin (modified from Crumière et al., 1990; Takashima et al., 2009): 1, Paleozoic crystalline rocks; 2, basin facies (black shales, marls and pelagic limestones); 3, shelf facies (sandstones, sandy bioclastic limestones); 4, carbonate platform facies (rudist bearing limestones); 5, Penninic thrust front; 6, Cretaceous fault; 7, 0-m isopach.

The investigated interval in the Lambruisse section is mainly composed of bedded white limestone and gray marl, although a 23-m interval of intercalated black shales and dark gray marls is present in the middle portion of the section. Takashima et al. (2009) described four main lithologic units in the Lambruisse section (Fig. 2), which are briefly described below.

The Upper Cenomanian Unit I is the lowest part of the studied section and is composed of gray marls with common intercalations of thin- to medium-bedded light gray calcareous marls. The overlying Unit II consists of alternating beds of limestone and light gray calcareous marl. Both Units I and II are strongly burrowed and contain many macro- and microfossils (Fig. 5A in Takashima et al., 2009). Unit III corresponds to the interval between the uppermost Cenomanian and the lowermost Turonian, and is correlated to the Thome Level (~OAE2; Crumière, 1990). In contrast to the previous units, the Thome Level is dominated by black shales and dark gray marls and is characterized by organic carbon-rich sediments. Based on lithofacies, Takashima et al. (2009) subdivided the Thome Level into 5 subunits (Fig. 2). Unit IV, which encompasses the Lower to Upper Turonian interval, consists of white-bedded limestones and a few intercalations of thin beds of dark gray marls and shales. The limestone beds are intensely burrowed and contain abundant microfossils such as radiolarians and planktonic and benthic foraminifers. Slumped limestone beds are frequently observed within this subunit. In the present study, only Units II–IV are investigated for calcareous nannofossils.

3. Material and methods

The present study investigates the calcareous nannofossil biostratigraphy of the 50-m interval across the C-T boundary of the Lambruisse section. A total of 57 samples were analyzed for calcareous nannofossils (Fig. 2). The Lambruisse section has been studied previously for lithology (Crumière et al., 1990), carbon isotope stratigraphy, TOC, calcium carbonate (CaCO_3) and planktonic foraminifer biostratigraphy (Takashima et al., 2009). Thus, the present study provides an opportunity to correlate these data with nannofossil biostratigraphy and, eventually, compare the result of the study with the C-T boundary sections in Pueblo (Western Interior Basin, USA), Bonarelli level in the Antriuiles (NE Italy), Eastbourne (UK) and Tarfaya sections (NW Africa).

For nannofossil biostratigraphic analysis, smear slides were prepared from the samples using the standard preparation technique (described in Bown and Young, 1998), and were examined under a light microscope using both cross-polarized light and phase contrast methods at $\times 1000$ to $\times 1600$ magnification. Calcareous nannofossil relative abundance categories were adopted from Bown et al. (1998) and Burnett et al. (1998). Additional fields of view (FOVs) were checked to verify rare occurrences of biostratigraphic marker species. The nannofossil biostratigraphic zones applied to the investigated section are the UC zones of Burnett et al. (1998). All nannofossil taxa observed in the studied section are listed in

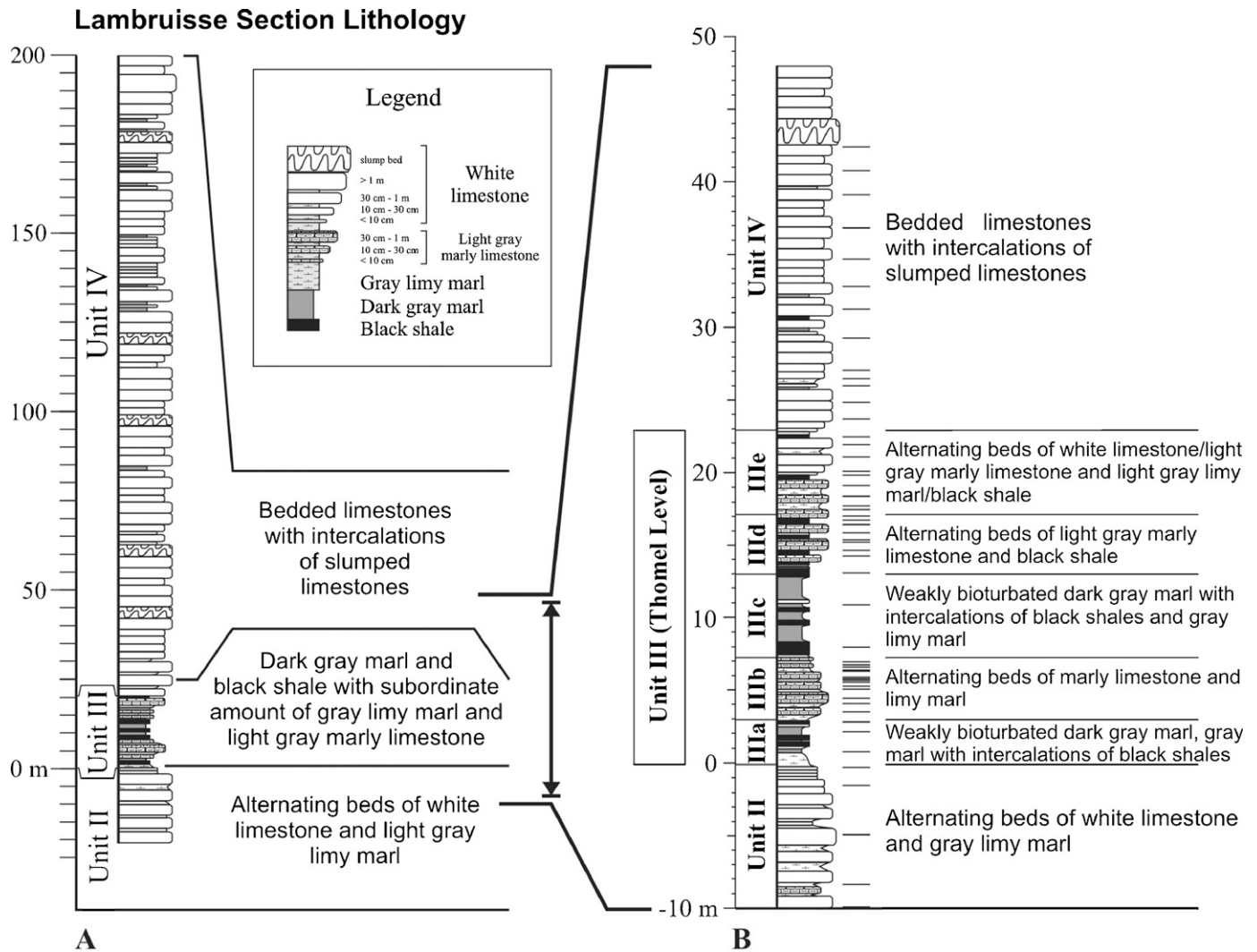


Fig. 2. **A.** Lithostratigraphy of the upper Cenomanian-upper Turonian succession in the Lambruisse section, Vocontian Basin. **B.** Detailed lithostratigraphy across the C-T boundary interval in the Lambruisse section. Short horizontal lines at the right of the section correspond to the samples investigated for nanofossils in the present study.

Appendix A. Microphotographs of selected nanofossil taxa are illustrated in Fig. 3.

4. Results

4.1. Calcareous nanofossils from the Lambruisse section

Nanofossils are generally few to abundant and are poorly to moderately-preserved. A total of 47 genera and 100 species were observed in the samples from the Lambruisse section (Appendix A). Most of the marker taxa, crucial in the delineation of the C-T boundary, were observed in the investigated samples (see Fig. 4). The sequence of these bioevents in the Lambruisse section is more or less comparable to previous studies across the C-T boundary interval in other sections (e.g., Bralower, 1988; Lamolda et al., 1997; Burnett et al., 1998; Luciani and Cobianchi, 1999; Paul et al., 1999; see discussion below).

The two bioevents used in the delineation of the C-T boundary in the present study, namely the last occurrence (LO) of *H. chiastia* and the first occurrence (FO) of *Q. gartneri*, as suggested in standard zonation schemes and in several studies (e.g., Sissingh, 1977; Perch-Nielsen, 1979, 1985; Bralower, 1988; Bralower et al., 1995; Lamolda et al., 1997; Burnett et al., 1998; Luciani and Cobianchi, 1999; Paul et al., 1999), occur less than 2 m apart, well defining the C-T boundary in the investigated section (Fig. 4). The LO of *H. chiastia* in the Lambruisse section, in addition, lies very close to the top of the carbon isotope excursion (i.e., end of the plateau of high $\delta^{13}\text{C}$ values) observed by Takashima et al. (2009; see Section 5.2).

4.2. Calcareous nanofossil biostratigraphy

Based on the stratigraphic distribution of the marker taxa (Fig. 4 and Appendix A), the investigated portion of the

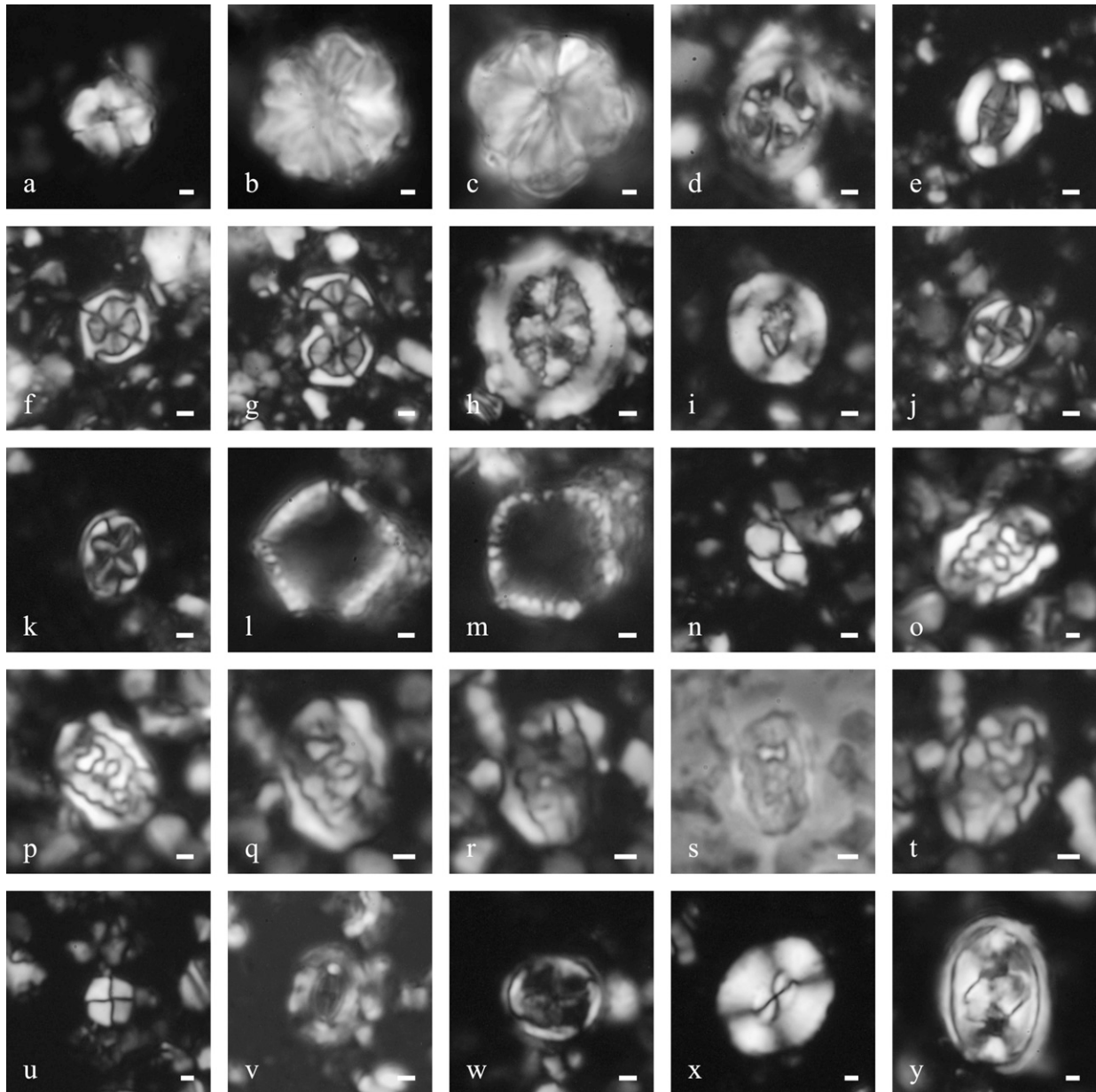


Fig. 3. Optical micrographs of calcareous nanofossils from the C-T boundary interval of the Lambruisse section, southeast France. All micrographs are crossed polar images except (s), which is phase contrast. **a.** *Assipetra* cf. *A. infracretacea*. LM-100; **b, c.** *A. terebrodentarius youngii*. LM-100 (b), LM-104 (c); **d.** *Axopodorhabdus albianus*. CT-051; **e.** *Broinsonia* cf. *B. enormis*. CT-039; **f, g.** *Corollithion kennedyi*. CT-052; **h.** *Cretarhabdus striatus*. LM-114; **i.** *Helenea chiasia*. CT-052; **j.** *Helicolithus compactus*. CT-039; **k.** *H. trabeculatus*. LM-104; **l, m.** *Laguncula montrisouensis*. LM-103; **n.** *Owenia* cf. *O. hillii*. CT-052; **o–t.** *Rhagodiscus* sp. CT-049; **u.** *Quadrum gartneri*. CT-039; **v.** *Sollasites horticus*. LM-103; **w.** *Stoverius achylosus*. LM-100; **x.** *Watznaueria barnesiae*. LM-103; **y.** *Zeugrhabdotus embergeri*. LM-104. Scale bar: 1 μ m.

Lambruisse section can be assigned to nanofossil zones UC3–UC8 zones (Middle Cenomanian to Middle Turonian). The resulting nanofossil biostratigraphy correlates well with the previously established planktonic foraminifer biostratigraphy in the section (Fig. 4).

4.2.1. UC3–UC4 undifferentiated zone (Middle–Upper Cenomanian)

The interval comprising the biostratigraphic range of *L. acutus* (CT-050 to LM-101) could not be subdivided, and thus corresponds to zones UC3 and UC4 of Burnett et al.

(1998). Small and large morphotypes of *Assipetra terebrodentarius* (i.e., spp. *terebrodentarius* and *youngii*) become common towards the upper part of the interval (Appendix A). *Acaenolithus cenomanicus* and *Corollithion kennedyi* are also present within the interval. The uppermost occurrences of the marker taxa *Axopodorhabdus albianus* and *Cretarhabdus striatus* were observed ~30 cm below the LO of *L. acutus* (Fig. 4). Other bioevents observed within the zone include the LO of *Braarudosphaera africana* and the occurrence of *Gartnerago theta* in one sample near the middle part of the interval (Fig. 4 and Appendix A).

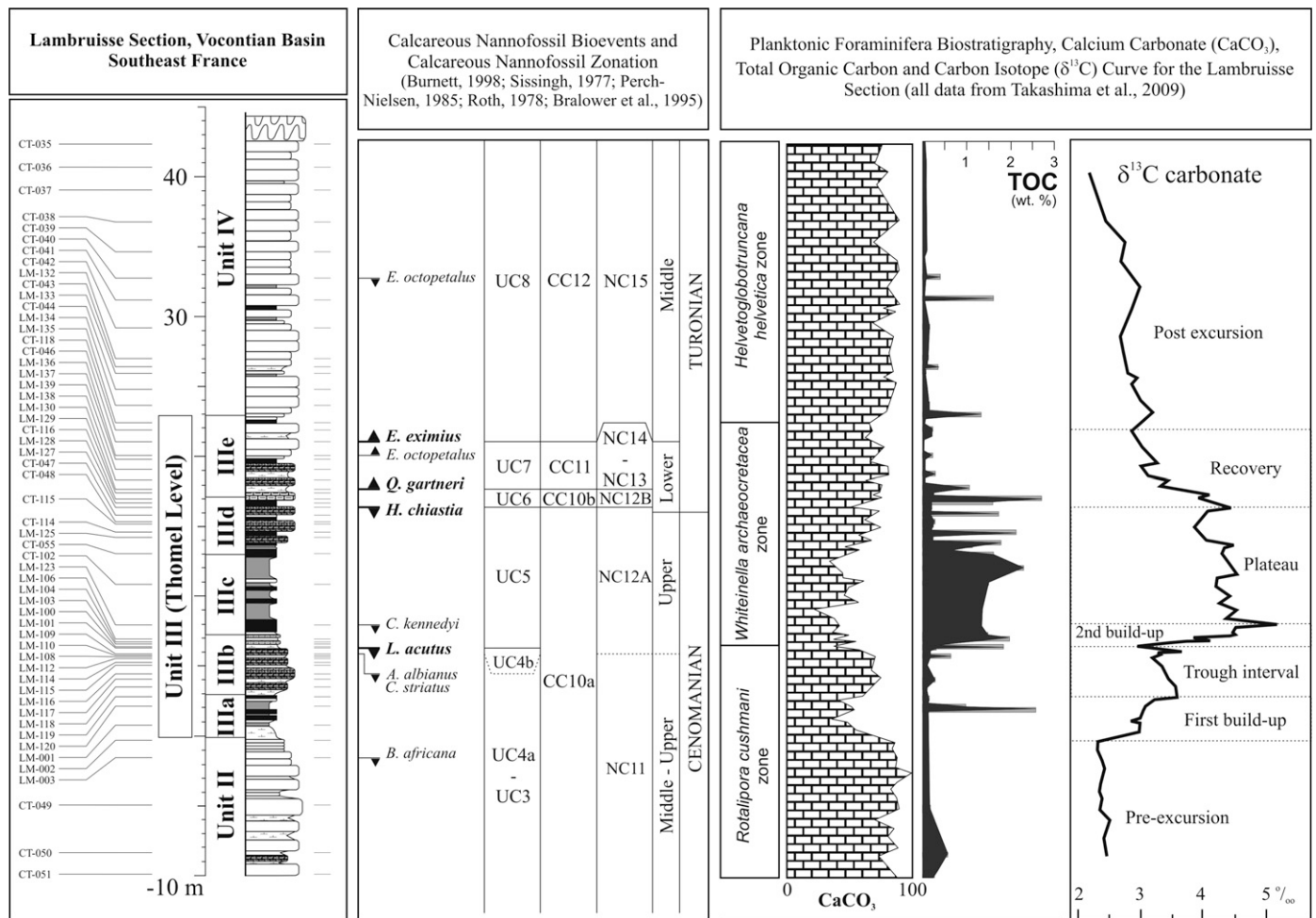


Fig. 4. Integrated calcareous nannofossil and planktonic foraminifer biostratigraphy, $\delta^{13}\text{C}$ profile/curve and TOC and CaCO_3 values across the C-T boundary interval in the Lambruisse section.

4.2.2. UC5 zone of Burnett et al. (1998; Upper Cenomanian-lowermost Turonian)

Includes the interval between the LO of *L. acutus* (LM-101) and the LO of *Helenea chiastia* (LM-127). The nannofossil assemblage is comparable to the previous zone, except that the relative abundances of some taxa are slightly reduced, either due to poor preservation (e.g., *Biscutum* spp. and *Discorhabdus ignotus*) or due to eutrophication event associated with OAE2 (e.g., *Broinsonia* spp., *Eprolithus floralis* and *Seribiscutum gaultensis*). This zone, in addition, is characterized by a (more) consistent occurrence of *Assipetra* spp. compared to the previous one (Appendix A). Bioevents observed within the interval include the LOs of *A. cenomanicus* and *C. kennedyi*. Following the UC zonation scheme of Burnett et al. (1998), the C-T boundary is delineated just below the LO of *H. chiastia*, within subunit IIIId of the Thomel Level (Fig. 4).

4.2.3. UC6 zone of Burnett et al. (1998; Lower Turonian)

The interval bounded by the LO of *H. chiastia* and the FO of *Quadrum gartneri* (LM-130). As mentioned previously, both taxa have been used in the delineation of the C-T boundary (Sissingh, 1977; Perch-Nielsen, 1979, 1985; Watkins, 1985 in

Kennedy and Cobban, 1991 and Kennedy et al., 2000; Bralower, 1988; Bralower et al., 1995; Bengtson, 1996; Lamolda et al., 1997; Burnett et al., 1998; Luciani and Cobianchi, 1999; Paul et al., 1999; Tsikos et al., 2004).

4.2.4. UC7 zone of Burnett et al. (1998; Lower Turonian)

The zone is the interval between the FO of *Q. gartneri* and the FO of *Eiffellithus eximius* (CT-046).

4.2.5. UC8 zone of Burnett et al. (1998; Lower-Middle Turonian)

The zone includes samples above the FO of *E. eximius*. The FO of *Eprolithus eptapetalus* and the LOs of *E. octopetalus* and *Rhagodiscus asper* were observed within the zone. Nannocoinids (i.e., *Nannoconus* spp. and *N. elongatus*) are also present within the lower part of the interval.

5. Discussion

Fig. 4 shows the integrated nannofossil and foraminifer biostratigraphy, carbon isotope curve and TOC and CaCO_3 values across the C-T boundary interval in the Lambruisse section.

5.1. Calcareous nannofossil bioevents

The sequence of nannofossil LOs and FOs across the investigated interval made it possible to establish a nannofossil zonation of the Lambruisse section, which has been studied previously by Takashima et al. (2009). In stratigraphical order, the following events were recorded in the section: (A) Cenomanian - LO *B. africana*, LO *A. albianus*, LO *C. striatus*, LO *L. acutus*, LO *A. cenomanicus* and LO *C. kennedyi*; (B) Turonian - LO *H. chiastia*, FO *Q. gartneri*, FO *E. octopetalus*, FO *E. eximius* and LO *E. octopetalus* (Fig. 4 and Appendix A). The C-T boundary in the studied section was delineated below the LO of *H. chiastia*, and this boundary is further constrained by the FO of *Q. gartneri* less than 2 m above (i.e., the C-T boundary in the Lambruisse section is within the UC5 nannofossil Zone and the *Whiteinella archaeocretacea* foraminifer Zone). Similarities and/or differences in the stratigraphic order of the bioevents in the Lambruisse section compared to other C-T boundary sections are shown in Fig. 5 and discussed below.

5.1.1. Cenomanian calcareous nannofossil bioevents

The Cenomanian bioevents in the Lambruisse section are consistent with the bioevents observed in other sections, indicating that the Upper Cenomanian sequence in the Lambruisse section is fairly complete. The sequence of the bioevents in the different sections, however, varies slightly (Fig. 5).

The LO of *C. kennedyi* is commonly reported to occur within the Upper Cenomanian (e.g., Bralower et al., 1995; Burnett et al., 1998). In the Lambruisse section, the LO of *C. kennedyi* was observed within the Upper Cenomanian UC5 zone, above the LOs of *A. albianus* and *L. acutus* (Fig. 4). Lamolda et al. (1997), Burnett et al. (1998) and Paul et al. (1999), however, reported the LO of *C. kennedyi* below the LOs of *L. acutus* and *A. albianus*. Luciani and Cobianchi (1999), conversely,

reported a much higher LO of *C. kennedyi* (above the C-T boundary; Fig. 5). Hardas and Mutterlose (2006) suggested differences in paleogeographic positions of the different sections as a probable cause for this pattern, although Luciani and Cobianchi (1999) attributed the younger LO of *C. kennedyi* in their study area (Italy) as the result of reworking.

In the Lambruisse section, the LO of *A. albianus* was observed within the UC3-UC4 undifferentiated zone (Upper Cenomanian), below the LO of *L. acutus* (Fig. 4). This succession of events is similar to the observations of Bralower (1988), Lamolda et al. (1997) and Paul et al. (1999), but differs from the standard zonation scheme of Burnett et al. (1998) and from the study of Luciani and Cobianchi (1999), wherein the LO of *A. albianus* was observed above the LO of *L. acutus* (Fig. 5). Bralower (1988) and Hardas and Mutterlose (2006) consider *A. albianus* as a reliable marker due to its continuous occurrence towards the end of its range. The LO of *A. albianus* in the Lambruisse section, therefore, probably represents a reliable event in the study area.

Other bioevents recorded in the Cenomanian of the Lambruisse section include the LOs of *B. africana* and *C. striatus* within the UC3-UC4 undifferentiated zone (Fig. 4). The LO of *B. africana* in the studied section is consistent with the observation of Luciani and Cobianchi (1999) who reported in their distribution chart (fig. 7, p. 144) the LO of the taxon within the lower part of the CC10a zone of Perch-Nielsen (1985), near the LO of *L. acutus*. Burnett et al. (1998), conversely, considered the LO of *B. africana* as a supplementary bioevent within the UC4 zone, between the FO of *Cylindralithus biarcus* and the LOs of *C. striatus* and *L. acutus*. *Braarudosphaera africana* is rare in the Lambruisse section samples. The apparent shorter range of *B. africana* in our section, therefore, could be the result of extreme scarcity of this taxon in the studied samples.

In the present study, the LO of *C. striatus* was observed below the LO of *L. acutus* (Fig. 4). This is similar to the

	Global Burnett et al. (1998) (UC Zonation Scheme)	Lambruisse section Vocontian Basin, SE France (this study)	Northern Italy Luciani and Cobianchi, 1999	Demerara Rise (Equatorial Atlantic) Hardas and Mutterlose, 2006	Eastbourne section England Paul et al., 1999	Tarfaya Basin Morocco Tsikos et al., 2004	Western Interior Basin Bralower, 1988	Northern Spain Lamolda et al., 1997
TURONIAN	▲ <i>E. eximius</i>	▼ <i>R. asper</i>	▲ <i>E. eximius</i>	▲ <i>E. eximius</i>			▼ <i>R. asper</i>	
	▲ <i>E. eptapetalus</i>	▲ <i>E. eptapetalus</i>	▲ <i>E. eptapetalus</i>	▲ <i>E. eptapetalus</i>				
CENOMANIAN	▲ <i>Q. gartneri</i>	▲ <i>E. eximius</i>	▲ <i>E. octopetalus</i>	▲ <i>E. octopetalus</i>	▲ <i>E. octopetalus</i>	▲ <i>E. octopetalus</i>		▲ <i>Q. gartneri</i>
	▲ <i>E. eptapetalus</i>	▲ <i>E. octopetalus</i>	▲ <i>Q. gartneri</i>	▲ <i>Q. gartneri</i>	▲ <i>Q. gartneri</i>	▲ <i>Q. gartneri</i>		▲ <i>E. octopetalus</i>
	▼ <i>H. chiastia</i>	▲ <i>Q. intermedium</i>	▲ <i>Q. intermedium</i>	▲ <i>Q. intermedium</i>	▲ <i>Q. intermedium</i>	▲ <i>Q. intermedium</i>		
	▲ <i>E. octopetalus</i>	▼ <i>Q. gartneri</i>	▼ <i>H. chiastia</i>	▼ <i>H. chiastia</i>	▼ <i>H. chiastia</i>	▲ <i>Q. gartneri</i>		
	▲ <i>Q. intermedium</i>	▼ <i>H. chiastia</i>	▼ <i>C. kennedyi</i>	▼ <i>C. kennedyi</i>	▼ <i>C. kennedyi</i>		▼ <i>H. chiastia</i>	▲ <i>Q. intermedium</i>
	▼ <i>R. asper</i>	▼ <i>C. kennedyi</i>	▼ <i>A. albianus</i>	▼ <i>A. albianus</i>	▼ <i>A. albianus</i>		▲ <i>E. eximius</i>	▼ <i>H. chiastia</i>
	▼ <i>A. albianus</i>	▼ <i>L. acutus</i>	▼ <i>R. asper</i>	▼ <i>R. asper</i>	▼ <i>R. asper</i>			
	▼ <i>L. acutus</i>	▼ <i>A. albianus</i>	▼ <i>L. acutus</i>	▼ <i>L. acutus</i>	▼ <i>L. acutus</i>		▼ <i>L. acutus</i>	▼ <i>L. acutus</i>
	▼ <i>C. striatus</i>	▼ <i>C. striatus</i>	▼ <i>C. striatus</i>	▼ <i>C. striatus</i>	▼ <i>C. striatus</i>		▼ <i>A. albianus</i>	▼ <i>A. albianus</i>
	▼ <i>B. africana</i>	▼ <i>C. striatus</i>	▲ <i>L. acutus</i>	▼ <i>C. kennedyi</i>	▼ <i>C. kennedyi</i>		▼ <i>C. kennedyi</i>	▼ <i>C. kennedyi</i>
▼ <i>C. kennedyi</i>	▼ <i>L. acutus</i>	▼ <i>C. striatus</i>		▼ <i>C. kennedyi</i>		▲ <i>Q. gartneri</i>		
▲ <i>L. acutus</i>								

Fig. 5. Comparison of the stratigraphic sequence of the nannofossil events between the Lambruisse section and other C-T boundary sections discussed in the paper (from Bralower, 1988; Lamolda et al., 1997; Burnett et al., 1998; Luciani and Cobianchi, 1999; Paul et al., 1999; Tsikos et al., 2004; Hardas and Mutterlose, 2006).

observations of Burnett et al. (1998) and Luciani and Cobianchi (1999; Fig. 5). The latter study, however, observed an earlier LO of *C. striatus*, before the FO of *L. acutus* and within the CC9c zone of Perch-Nielsen (1985). Burnett et al. (1998) considers the LO of *C. striatus* as a supplementary bioevent within the Upper Cenomanian, marking the base of the UC4b subzone. The LO of *C. striatus* in the section, however, coincides with the LO of *A. albianus* (Fig. 4). The presence of an unconformity in the section may be indicated by this observation, although it is unlikely the case due to the presence of *L. acutus* above the two taxa. Takashima et al. (2009), in addition, did not indicate the presence of an unconformity in the section, although Crumière (1991) mentioned the presence of “hiatus” in the Lambruisse section, near the boundary of the *Rotalipora cushmani* and *W. archaeocretacea* planktonic foraminifer Zones. Another possible reason for our record could be the poor preservation of nannofossils in the Lambruisse section, which makes it difficult sometimes to identify some specimens with a certain degree of confidence.

5.1.2. C-T boundary calcareous nannofossil bioevents

Calcareous nannofossil biostratigraphic resolution across the C-T boundary has been greatly improved in the last decade, as indicated by the number of published works in several sections worldwide. Despite this, there seems to be disagreement among authors as to what nannofossil event(s) should be used to delineate the C-T boundary (Fig. 5). Calcareous nannofossil markers commonly used in delineating the C-T boundary include the LOs of *A. albianus* and *H. (= Microstaurus) chiastia* and the FO of *Q. gartneri*. Although the order of these bioevents slightly varies between different authors, these marker taxa have already been recognized and used in a number of sections in Europe (England, Italy and Spain), North America, Jordan, Africa and in the equatorial Atlantic (e.g., Bralower, 1988; Jarvis et al., 1988; Lamolda et al., 1997; Luciani and Cobianchi, 1999; Paul et al., 1999; Premoli Silva et al., 1999; Gale et al., 2000; Bauer et al., 2001; Erba, 2004; Schulze et al., 2004; Hardas and Mutterlose, 2006, 2007). Additional nannofossil events across the C-T boundary include the FOs of *Q. intermedium*, *E. octopetalus* and *E. eptapetalus* (Fig. 5; Varol, 1992; Lamolda et al., 1997; Burnett et al., 1998; Luciani and Cobianchi, 1999; Paul et al., 1999; Hardas and Mutterlose, 2006).

In the Lambruisse section, as mentioned previously, the C-T boundary was detected below the LO of *H. chiastia* and the FO of *Q. gartneri* (Fig. 4). The LO of *H. chiastia* is one of the most important markers for the Upper Cenomanian (Perch-Nielsen, 1979, 1985; Lamolda et al., 1997; Paul et al., 1999). This LO has already been used as a C-T boundary marker in the studies of Bralower (1988), Bralower et al. (1995), and Luciani and Cobianchi (1999). In the UC zonation scheme of Burnett et al. (1998), the LO of *H. chiastia* occurs immediately above the C-T boundary. The use of the FO of *Q. gartneri* as the C-T boundary marker, on the other hand, had also been applied in several studies as well (e.g., Sissingh, 1977; Perch-Nielsen, 1979, 1985; Watkins, 1985 in Kennedy and Cobban, 1991 and Kennedy et al., 2000; Varol, 1992; Bengtson, 1996; Tsikos

et al., 2004; Kolonic et al., 2005). In the Pueblo stratotype section, this event occurs within the *W. devonense* ammonite Zone. Bralower (1988), however, found the taxon at a lower stratigraphic level, within the *Metoicoceras mosbyense* ammonite Zone (Upper Cenomanian). Burnett et al. (1998), in addition, indicated the FO of *Q. gartneri* within the Lower Turonian, similar to the work of Luciani and Cobianchi (1999).

5.1.3. Turonian calcareous nannofossil bioevents

Above the FO of *Q. gartneri*, the following bioevents were observed in the Lambruisse section (in stratigraphical order): FO *E. octopetalus*, FO *E. eximius*, FO *E. eptapetalus* and LO *E. octopetalus* (Fig. 4 and Appendix A). All these bioevents are considered to be Early to Middle Turonian in age by Burnett et al. (1998).

The FO of *E. octopetalus* has already been recognized and used as a C-T boundary marker in several studies (e.g., Varol, 1992; Lamolda et al., 1997). In the Lambruisse section, the FO of *E. octopetalus* was observed above the FO of *Q. gartneri* and below the FO of *E. eximius* (Fig. 4). Burnett et al. (1998) and Lamolda et al. (1997), however, placed the event before the FO of *Q. gartneri*, just above the C-T boundary (Fig. 5). Nevertheless, the observation in the Lambruisse section is similar to the observations in Italy (Luciani and Cobianchi, 1999), Eastbourne section in UK (Paul et al., 1999), and in Demerara Rise (equatorial Atlantic; Hardas and Mutterlose, 2006).

The FO of *Q. intermedium*, another taxon used in the delineation of the C-T boundary, is observed in this work between the FO of *Q. gartneri* and the FO of *E. octopetalus* (UC7 zone; Fig. 5 and Appendix A). Luciani and Cobianchi (1999) and Paul et al. (1999) recognize this event above the C-T boundary, below the FOs of *Q. gartneri* and *E. octopetalus* (Fig. 5). Lamolda et al. (1997), Burnett et al. (1998) and Hardas and Mutterlose (2006), conversely, observed the FO of *Q. intermedium* within the Upper Cenomanian (UC5c subzone of Burnett et al., 1998). The discrepancies in the timing of this bioevent could be due to paleogeographic differences of the sections investigated by the authors, although preservational problems could also play a role, as in the case of the present study where *Q. intermedium* is rare and its occurrence discontinuous.

The FO of *E. eximius* above the FO of *Q. gartneri* defines the base of the UC8 nannofossil zone and the base of the Middle Turonian (Fig. 4 and Appendix A). The succession of these two bioevents is consistent with the zonation schemes of Roth (1978), Perch-Nielsen (1979, 1985) and Burnett et al. (1998), and the studies of Luciani and Cobianchi (1999) in NE Italy and Hardas and Mutterlose (2006) in the equatorial Atlantic (Fig. 5). The FO of *E. eximius* in the Lambruisse section, however, is very close to the C-T boundary, suggesting the possibility that part of the Lower Turonian is either missing or condensed, although the $\delta^{13}\text{C}$ profile and the planktonic foraminifer biostratigraphy (Takashima et al., 2009) do not indicate condensation. Interestingly, a similar record has been reported by Hardas and Mutterlose (2006) in Demerara Rise. Bralower (1988) also observed the FO of *E. eximius* above the

FO of *Q. gartneri*, although both events are within the Upper Cenomanian. The discrepancies in the timing of the FO of *E. eximius*, among other reasons, can be due to different taxonomic concepts among nannofossil biostratigraphies.

The FO of *E. eptapetalus* and the LO of *E. octopetalus* in the Lambruisse section were observed above the FO of *E. eximius*. The position of the FO of *E. eptapetalus* with respect to other bioevents varies among authors. In the study of **Luciani and Cobianchi (1999)** and **Hardas and Mutterlose (2006)**, the FO of the taxon was observed between the FOs of *E. octopetalus* and *E. eximius* (Lower Turonian; Fig. 5). In **Burnett et al. (1998)**, on the other hand, this bioevent was observed between the LO of *H. chiastia* and the FO of *Q. gartneri* (Lower Turonian). **Varol (1992)**, however, observed the FO of *E. eptapetalus* within the Upper Cenomanian.

5.2. Correlation of nannofossil and planktonic foraminifer biostratigraphies, TOC, CaCO₃ and carbon isotope

Takashima et al. (2009) investigated the planktonic foraminifer biostratigraphy, carbon isotope, TOC and CaCO₃ values across the C-T boundary interval in the Lambruisse section. The comparison of these data with respect to the nannofossil zones established in this study is shown in Fig. 4. Comparison of the Lambruisse section with the Eastbourne and Pueblo reference sections is shown in Fig. 6.

Based on the LO of *Rotalipora cushmani* and the FO of *Helvetoglobotruncana helvetica*, the *R. cushmani*, *W. archaeocretacea* and *H. helvetica* foraminifer Zones were recognized in the Lambruisse section (**Takashima et al., 2009**). The LO of *A. albianus* occurs before the LO of *R. cushmani* (i.e.,

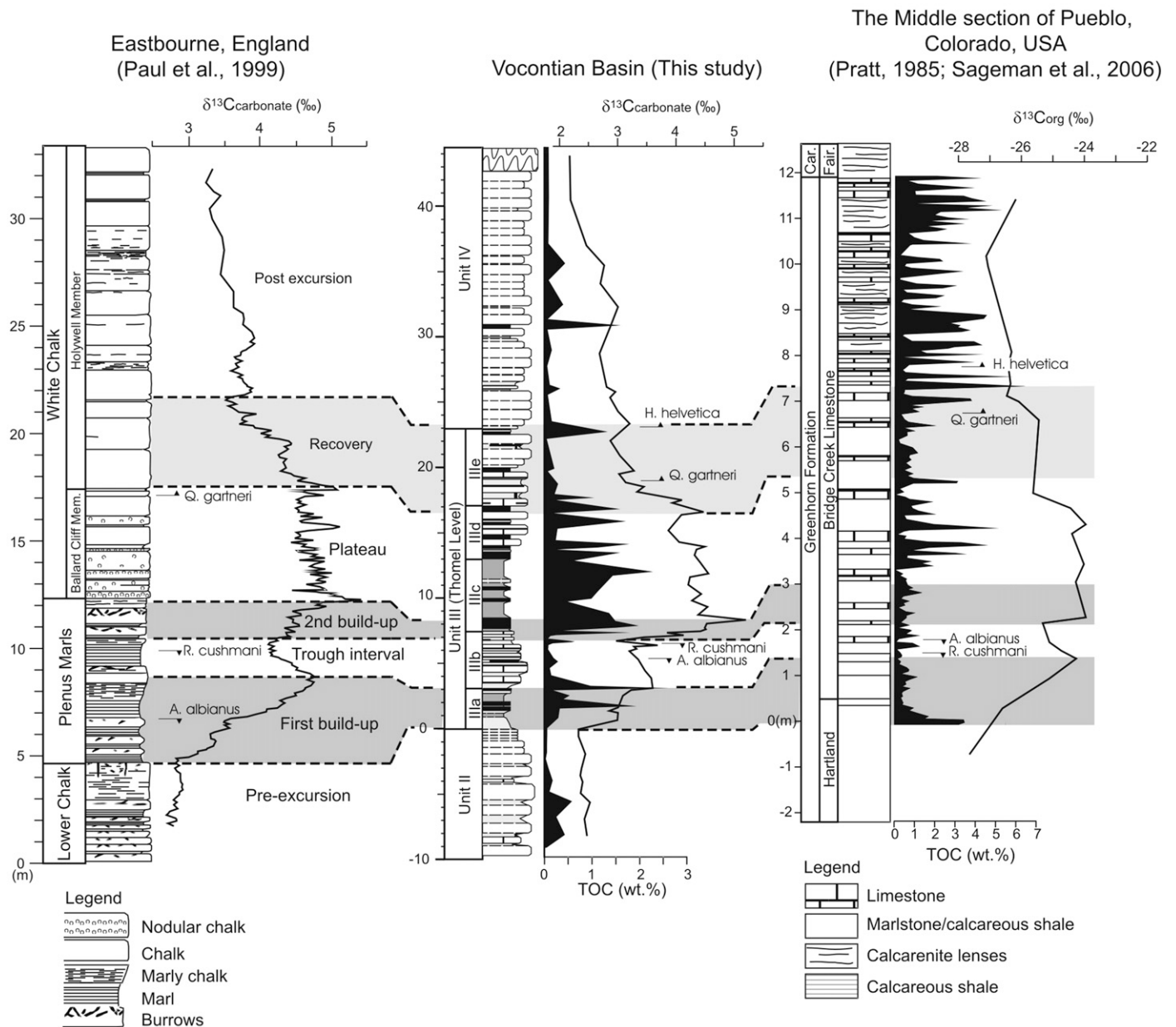


Fig. 6. Correlation of the C-T boundary interval between the Lambruisse section (Vocontian Basin) and the Eastbourne (England) and Pueblo (USA) reference sections (adapted from **Takashima et al., 2009**).

within the *R. cushmani* Zone) and the FO of *Q. gartneri* occurs before the FO of *H. helvetica* (i.e., within the *W. archaeocretacea* Zone). These observations in the Lambruisse section are comparable to the observed succession in Eastbourne, UK (Paul et al., 1999), Tarfaya, Morocco (Tsikos et al., 2004) and northern Spain (Lamolda et al., 1997). Luciani and Cobianchi (1999) observed a coincidence in the timing of the LOs of *A. albianus* and *R. cushmani* and the FOs of *Q. gartneri* and *H. helvetica*. In the Pueblo stratotype section, the LO of *A. albianus* is above the LO of *R. cushmani*. Basically, the nannofossil biostratigraphy correlates well with the planktonic foraminifer biostratigraphy, except for the *H. helvetica* Zone, which is inconsistent with previous studies (e.g., Gradstein et al., 2004). This problem is due to the early FO of *E. eximius* in the Lambruisse section, as it was discussed in section 5.1.3.

Paul et al. (1999) recognized seven phases based on $\delta^{13}\text{C}$ profile fluctuations in the Eastbourne section (Fig. 6):

- pre-excursion phase with low $\delta^{13}\text{C}$ values;
- first build-up, characterized by distinct rise in $\delta^{13}\text{C}$;
- trough interval with low $\delta^{13}\text{C}$ values;
- second $\delta^{13}\text{C}$ build-up;
- plateau of high $\delta^{13}\text{C}$ values;
- recovery, characterized by gradual decline of $\delta^{13}\text{C}$ values;
- post-excursion phase with a gentle decline in $\delta^{13}\text{C}$ values.

The $\delta^{13}\text{C}$ profile in the Lambruisse section (Takashima et al., 2009) closely follows and correlates well with the Eastbourne section (Fig. 6).

Detailed chemostratigraphic analysis of the Lambruisse section by Takashima et al. (2009) indicates that the $\delta^{13}\text{C}$ profile of the section corresponds well with changes in lithofacies and fluctuations in the TOC and CaCO_3 content (Fig. 4). Initial increase in the $\delta^{13}\text{C}$ values (first build-up) occurs within UC3-UC4a (Middle to Upper Cenomanian), coinciding with the onset of the deposition of the organic-rich sediments of the Thomel Level (OAE2) and significant decline in the CaCO_3 values. Within the “trough interval” and before the 2nd $\delta^{13}\text{C}$ build-up, which is also within UC3-UC4a, the LOs of the nannofossil *A. albianus*, *C. striatus*, *L. acutus* and of the planktonic foraminifer *R. cushmani* were observed. The LOs of *A. albianus* and *R. cushmani* were also observed within the “trough interval” in the Pueblo section, although at reversed stratigraphic positions with respect to the observation in the Lambruisse section (Fig. 6). In the Eastbourne section, the LO of *A. albianus* occurs within the “first build-up” interval.

The plateau of high $\delta^{13}\text{C}$ values (i.e., positive $\delta^{13}\text{C}$ excursion), conversely, occurs within UC5 (Upper Cenomanian to lowermost Cenomanian), between the LO of *C. kennedyi* and the LO of *H. chiastia*. This interval of high $\delta^{13}\text{C}$ values corresponds to the Thomel Level (OAE2), which is also characterized by high TOC and low CaCO_3 values (Fig. 4). Slightly below the end of the plateau of high $\delta^{13}\text{C}$ values lies the C-T boundary, that was delineated using the LO of *H. chiastia*. This level also marks the end of consistent high TOC values and the base of UC6. The position of the C-T boundary in the Lambruisse section with respect to the carbon isotope excursion

(i.e., end of the $\delta^{13}\text{C}$ plateau) is similar to the observation in the Eastbourne section (UK; Gale et al., 2000) and comparable to the observation in the Wunstorf section (North Germany), where the C-T boundary (defined using the base of the ammonite *Watinoceras*) coincides with the end of the plateau phase of the carbon isotope excursion (Voigt et al., 2008).

The FO of *Q. gartneri* occurs immediately above the plateau of high $\delta^{13}\text{C}$ values, within the “recovery” phase/interval of the isotope curve. As mentioned in section 5.1.2, the LO of *H. chiastia* and FO of *Q. gartneri* were used to delineate the C-T boundary in the Lambruisse section. Tsikos et al. (2004) consider the FO of *Q. gartneri* as a useful datum level for the C-T boundary and, because of its proximity to the end of the plateau of high $\delta^{13}\text{C}$ values, as a marker for the end of the OAE2. Lees (2002) indicates the start and end of the OAE2 near the LO of *C. kennedyi* and the FO of *Q. gartneri*, respectively. Interestingly, the plateau of high $\delta^{13}\text{C}$ values in the Lambruisse section occurs between these two bioevents (Fig. 4). Near the base of the *H. helvetica*, within the lower part of UC8 (Lower to Middle Turonian), the $\delta^{13}\text{C}$ curve returns to pre-excursion values.

6. Summary and conclusions

Calcareous nannofossil biostratigraphic analysis of the Lambruisse section in the Vocontian Basin resulted to the recognition of several nannofossil bioevents crucial in the establishment of the nannofossil zones and delineation of the C-T boundary in the section. Based on the stratigraphic distributions of the marker taxa (i.e., *A. albianus*, *C. striatus*, *L. acutus*, *C. kennedyi*, *H. chiastia*, *Q. gartneri*, *E. octopetalus*, *E. eximius* and *E. eptapetalus*), the investigated portion of the Lambruisse section was assigned to nannofossil zones UC3-UC8, encompassing the Middle Cenomanian to Middle Turonian interval.

With the establishment of the nannofossil biostratigraphy in the Lambruisse section, relative timing of events like the $\delta^{13}\text{C}$ excursion, TOC and carbonate fluctuations is determined. This provides valuable biostratigraphic and chemostratigraphic framework for the Lambruisse section, which enabled correlation with other C-T boundary sections, such as the Pueblo stratotype section in the Western Interior Basin (US) and the Eastbourne section (UK). Correlation with the Wunstorf section (North Germany), which is a reference section for the C-T boundary, is also promising. Comparison between the different C-T boundary sections revealed that the C-T boundary interval in the Lambruisse section is as complete as in the other sections, in terms of nannofossil biostratigraphy and $\delta^{13}\text{C}$ stratigraphy. Minor differences include the timing and succession of several nannofossil bioevents, which could be due to preservational artifacts and differences in taxonomic concepts and paleogeographic positions of the sections.

Acknowledgements

A.G.S. Fernando started the research while still at Hokkaido University under the Monbukagakusho Scholarship Program. The study was also supported by the 21st Century COE

Program “The Neoscience of Natural History” of Hokkaido University. The author completed the research at the National Institute of Geological Sciences under the 2007 NIGS Research Grant. The paper was presented at the 12th INA Conference in Lyon, France in 2008 with support from the Commission on Higher Education (CHED) and INA12 Organizing Committee. Authors thank Jens Herrle, Jackie Lees and Emanuela Mattioli for reviewing the initial draft and for their helpful comments and suggestions.

Appendix A. Supplementary data

Supplementary data associated with this article can be found, in the online version, at doi:10.1016/j.geobios.2009.11.003.

References

- Bauer, J., Marzouk, A.M., Steuber, T., Kuss, J., 2001. Lithostratigraphy and biostratigraphy of the Cenomanian-Santonian strata of Sinai, Egypt. *Cretaceous Research* 22, 497–526.
- Bengtson, P., 1996. The Turonian stage and substage boundaries. In: Rawson, P.F., Dhondt, A.V., Hancock, J.M., Kennedy, W.J. (Eds.), *Proceedings of the Second International Symposium on Cretaceous Stage Boundaries*. Bulletin de l’Institut Royal des Sciences Naturelles de Belgique, Sciences de la Terre 66 (supplément), pp. 69–79.
- Bornemann, A., Pross, J., Reichelt, K., Herrle, J.O., Hemleben, C., Mutterlose, J., 2005. Reconstruction of short-term palaeoceanographic changes during the formation of the late Albian “Niveau Breistroffer” black shales (Oceanic Anoxic Event 1d, SE France). *Journal of the Geological Society, London* 162, 623–639.
- Bown, P.R., Rutledge, D.C., Crux, J.A., Gallagher, L.T., 1998. Lower Cretaceous. In: Bown, P.R. (Ed.), *Calcareous Nannofossil Biostratigraphy*. British Micropalaeontological Society Publications Series. Chapman and Hall/Kluwer Academic Publishers, pp. 86–131.
- Bown, P.R., Young, J.R., 1998. Techniques. In: Bown, P.R. (Ed.), *Calcareous Nannofossil Biostratigraphy*. British Micropalaeontological Society Publications Series. Chapman and Hall/Kluwer Academic Publishers, pp. 16–28.
- Bralower, T.J., 1988. Calcareous nannofossil biostratigraphy and assemblages of the Cenomanian-Turonian boundary interval: implications for the origin and timing of oceanic anoxia. *Paleoceanography* 3, 275–316.
- Bralower, T.J., Fullagar, P.D., Paull, C.K., Dwyer, G.S., Leckie, R.M., 1997. Mid Cretaceous strontium-isotope stratigraphy of deep-sea sections. *Geological Society of America Bulletin* 109, 1421–1442.
- Bralower, T.J., Leckie, R.M., Sliter, W.V., Thierstein, H.R., 1995. An integrated Cretaceous microfossil biostratigraphy. In: Berggren, W.A., Kent, D.V., Aubry, M.P., Hardenbol, J. (Eds.), *Geochronology, Time Scales and Global Stratigraphic Correlation*. SEPM Special Publication, pp. 65–79.
- Burnett, J.A., Gallagher, L.T., Hampton, M.J., 1998. Upper Cretaceous. In: Bown, P.R. (Ed.), *Calcareous nannofossil biostratigraphy*. British Micropalaeontological Society Publications Series. Chapman and Hall/Kluwer Academic Publishers, pp. 132–199.
- Cotillon, P., Rio, M., 1984. Cyclic sedimentation in the Cretaceous of Deep Sea Drilling Project sites 535 and 540 (Gulf of Mexico), 534 (central Atlantic) and in the Vocontian Basin (France). In: Buffler, P., Schlager, W. (Eds.), *Initial Reports of the Deep Sea Drilling Project 77*. US Government Printing Office, Washington, pp. 339–376.
- Crumière, J.P., 1990. Crise anoxique à la limite Cénoomanien-Turonien dans le bassin subalpin oriental (Sud-Est de la France) : Relation avec l’eustatisme. In : Cotillon, P. (Ed.), *Les événements de la partie moyenne du Crétacé (Aptien à Turonien)*. *Geobios* MS 11, pp. 189–203.
- Crumière, J.P., 1991. The Cenomanian-Turonian Oceanic Anoxic Event (CTOAE) in the Southern Subalpine Domain (Northwestern Tethyan Margin, South-east of France). *Excursion dans le SE de la France (Guide)*, 9–56.
- Crumière, J.P., Crumière-Airaud, C., Espitalié, J., Cotillon, P., 1990. Global and regional controls on potential source-rock deposition and preservation: the Cenomanian-Turonian oceanic anoxic event on the European Tethyan margin (SE France). In: Huc, A.Y. (Ed.), *Deposition of organic facies*, 30. American Association of Petroleum Geologists, Studies in Geology, Tulsa, pp. 107–118.
- Duchamp-Alphonse, S., Gardin, S., Fiet, N., Bartolini, A., Blamart, D., Pagel, M., 2007. Fertilization of the northwestern Tethys (Vocontian basin, SE France) during the Valanginian carbon isotope perturbation: Evidence from calcareous nannofossils and trace element data. *Palaeogeography Palaeoclimatology Palaeoecology* 243, 132–151.
- Duncan, R.A., Bralower, T.J., 2002. Environmental and biotic consequences of large igneous provinces. In: Bice, K.L., et al. (Eds.), *Cretaceous Climate-Ocean Dynamics: Future Directions for IODP*. http://www.who.edu/ccod/CCOD_report.html.
- Erba, E., 2004. Calcareous nannofossils and Mesozoic anoxic events. *Marine Micropaleontology* 52, 85–106.
- Erbacher, J., Hemleben, C., Huber, B.T., Markey, M., 1999. Correlating environmental changes during early Albian oceanic anoxic event 1B using benthic foraminiferal paleoecology. *Marine Micropaleontology* 38, 7–28.
- Erbacher, J., Thurow, J., Littke, R., 1996. Evolution patterns of radiolaria and organic matter variations: A new approach to identify sea-level changes in mid-Cretaceous pelagic environments. *Geology* 24, 499–502.
- Fries, G., Parize, O., 2003. Anatomy of ancient passive margin slope systems: Aptian gravity-driven deposition on the Vocontian palaeomargin, western Alps, South-East France. *Sedimentology* 50, 1231–1270.
- Gale, A.S., Jenkyns, H.C., Kennedy, W.J., Corfield, R.M., 1993. Chemostratigraphy versus biostratigraphy: data from around the Cenomanian-Turonian boundary. *Journal of the Geological Society, London* 150, 29–32.
- Gale, A.S., Smith, A.B., Monks, N.E.A., Young, J.A., Howard, A., Wray, D.S., Huggett, J.M., 2000. Marine biodiversity through the Late Cenomanian-Early Turonian: paleoceanographic controls and sequence stratigraphic biases. *Journal of the Geological Society, London* 157, 745–757.
- Giraud, F., Olivero, D., Baudin, F., Reboulet, S., Pittet, B., Proux, O., 2003. Minor changes in surface-water fertility across the oceanic anoxic event 1d (latest Albian, SE France) evidenced by calcareous nannofossils. *International Journal of Earth Sciences* 92, 267–284.
- Gradstein, F.M., Ogg, J.G., Smith, A.G. (Eds.), 2004. *A Geologic Time Scale*. Cambridge University Press, Cambridge.
- Grosheny, D., Beaudoin, B., Morel, L., Desmares, D., 2006. High-resolution biostratigraphy and chemostratigraphy of the Cenomanian/Turonian boundary event in the Vocontian Basin, southeast France. *Cretaceous Research* 27, 629–640.
- Grosheny, D., Tronchetti, G., 1993. La crise Cénoomanien-Turonien : réponse comparée des assemblages de foraminifères benthiques de plate-forme carbonatée et de bassin dans le Sud-Est de la France. *Cretaceous Research* 14, 397–408.
- Hardas, P., Mutterlose, J., 2006. Calcareous nannofossil biostratigraphy of the Cenomanian/Turonian boundary interval of ODP Leg 207 at the Demerara Rise. *Revue de Micropaleontologie* 29, 165–179.
- Hardas, P., Mutterlose, J., 2007. Calcareous nannofossil assemblages of Oceanic Anoxic Event 2 in the equatorial Atlantic: Evidence of an eutrophication event. *Marine Micropaleontology* 66, 52–69.
- Hasegawa, T., 1997. Cenomanian-Turonian carbon isotope events recorded in terrestrial organic matter from northern Japan. *Palaeogeography Palaeoclimatology Palaeoecology* 130, 251–273.
- Hay, W.W., DeConto, R.M., Wold, C.N., Wilson, K.M., Voigt, S., Schulz, M., Rossby Wold, A., Dullo, W.C., Ronov, A.B., Balukhovskiy, A.N., Söding, E., 1999. Alternative global Cretaceous paleogeography. In: Barrera, E., Johnson, C.C. (Eds.), *Evolution of the Cretaceous Ocean-Climate System*. The Geological Society of America Special Paper 332, Boulder, pp. 1–47.
- Heimhofer, U., Hochuli, P.A., Herrle, J.O., Weissert, H., 2006. Contrasting origins of Early Cretaceous black shales in the Vocontian basin: Evidence from palynological and calcareous nannofossil records. *Palaeogeography Palaeoclimatology Palaeoecology* 235, 93–109.
- Herrle, J.O., 2002. Mid-Cretaceous paleoceanographic and paleoclimatologic implications on black shale formation of the Vocontian Basin and Atlantic:

- Evidence from calcareous nannofossils and stable isotopes. *Tübinger Mikropaläontologische Mitteilungen* 27, 1–114.
- Herrle, J.O., 2003. Reconstructing nutricline dynamics of mid-Cretaceous oceans: evidence from calcareous nannofossils from the Niveau Paquier black shale (SE France). *Marine Micropaleontology* 47, 307–321.
- Herrle, J.O., Mutterlose, J., 2003. Calcareous nannofossils from the Aptian-Lower Albian of southeast France: palaeoecological and biostratigraphic implications. *Cretaceous Research* 24, 1–22.
- Herrle, J.O., Pross, J., Friedrich, O., Köbber, P., Hemleben, C., 2003. Forcing mechanisms for mid-Cretaceous black shale formation: evidence from the Upper Aptian and Lower Albian of the Vocontian Basin (SE France). *Palaeogeography Palaeoclimatology Palaeoecology* 190, 399–426.
- Holbourn, A., Kuhnt, W., Erbacher, J., 2001. Benthic foraminifers from Lower Albian black shales (Site 1049, ODP Leg 171): Evidence for a non “uniformitarian” record. *Journal of Foraminiferal Research* 31, 60–74.
- Jarvis, I., Carson, G.A., Cooper, M.K.E., Hart, M.B., Leary, P.N., Tocher, B.A., Horne, D., Rosenfeld, A., 1988. Microfossil Assemblages and the Cenomanian-Turonian (late Cretaceous) Oceanic Anoxic Event. *Cretaceous Research* 9, 3–103.
- Jenkyns, H.C., Gale, A.S., Corfield, R.M., 1994. Carbon- and oxygen-isotope stratigraphy of the English Chalk and Italian Scaglia and its palaeoclimatic significance. *Geological Magazine* 131, 1–34.
- Joseph, P., Beaudoin, B., Fries, G., Parize, O., 1989. Les vallées sous-marines enregistrées au Crétacé inférieur le fonctionnement en blocs basculés du domaine vocontien. *Comptes Rendus de l'Académie des Sciences de Paris* 309, 1031–1038.
- Kennedy, W.J., Cobban, W.A., 1991. Stratigraphy and interregional correlation of the Cenomanian-Turonian transition in the Western Interior of the United States near Pueblo, Colorado, a potential boundary stratotype for the base of the Turonian stage. *Newsletter on Stratigraphy* 24, 1–33.
- Kennedy, W.J., Walaszczyk, I., Cobban, W.A., 2000. Pueblo, Colorado, USA, candidate Global Boundary Stratotype Section and Point for the base of the Turonian Stage of the Cretaceous, and for the base of the Middle Turonian Substage, with a revision of the Inoceramidae (Bivalvia). *Acta Geologica Polonica* 50, 295–334.
- Kolonik, S., Wagner, T., Forster, A., Sinninghe Damste, J.S., Walsworth-Bell, B., Erba, E., Turgeon, S., Brumsack, H.J., Chellai, E.H., Tsikos, H., Kuhnt, W., Kuypers, M.M.M., 2005. Black shale deposition on the northwest African Shelf during the Cenomanian/Turonian oceanic anoxic event: Climate coupling and global organic carbon burial. *Paleoceanography* 20, 1006, doi:10.1029/2003PA000950.
- Kuypers, M.M.M., Pancost, R.D., Nijenhuis, I.A., Sinninghe Damste, J.S., 2002. Enhanced productivity led to increased organic carbon burial in the euxinic North Atlantic basin during the late Cenomanian oceanic anoxic event. *Paleoceanography* 17, 1051, doi:10.1029/2000PA000659.
- Kuypers, M.M.M., Pancost, R.D., Sinninghe Damste, J.S., 1999. A large and abrupt fall in atmospheric CO₂ concentration during Cretaceous times. *Nature* 399, 342–345.
- Lamolda, M.A., Gorostidi, A., Martinez, R., Lopez, G., Peryt, D., 1997. Fossil occurrences in the Upper Cenomanian-Lower Turonian at Ganuza, northern Spain: an approach to Cenomanian/Turonian boundary chronostratigraphy. *Cretaceous Research* 18, 331–353.
- Leckie, R.M., Bralower, T.J., Cashman, R., 2002. Oceanic anoxic events and plankton evolution: Biotic response to tectonic forcing during the mid-Cretaceous. *Paleoceanography* 17, 3, doi:10.1029/2001PA000623.
- Lees, J.A., 2002. Calcareous nannofossil biogeography illustrates palaeoclimate change in the Late Cretaceous Indian Ocean. *Cretaceous Research* 23, 537–634.
- Luciani, V., Cobianchi, M., 1999. The Bonarelli Level and other black shales in the Cenomanian-Turonian of the northeastern Dolomites (Italy): calcareous nannofossil and foraminiferal data. *Cretaceous Research* 20, 135–167.
- Paul, C.R.C., Lamolda, M.A., Mitchell, S.F., Vaziri, M.R., Gorostidi, A., Marshall, J.D., 1999. The Cenomanian-Turonian boundary at Eastbourne (Sussex, UK): a proposed European reference section. *Palaeogeography Palaeoclimatology Palaeoecology* 150, 83–121.
- Perch-Nielsen, K., 1979. Calcareous nannofossils from the Cretaceous between the North Sea and the Mediterranean. In: Wiedmann, J. (Ed.), *Aspekte der Kreide Europas IUGS A6*, 223–272.
- Perch-Nielsen, K., 1985. Mesozoic Calcareous Nannofossils. In: Bolli, H.M., Saunders, J.B., Perch-Nielsen, K. (Eds.), *Plankton Stratigraphy*. Cambridge University Press, Cambridge, pp. 17–86.
- Pratt, L.M., Threlkeld, C.N., 1984. Stratigraphic significance of ¹³C/¹²C ratios in mid-Cretaceous rocks of the Western Interior, USA. In: Stott, D.F., Glass, D.J. (Eds.), *The Mesozoic of Middle North America*. Canadian Society of Petroleum Geologists Memoir 9, pp. 305–312.
- Premoli Silva, I., Erba, E., Salvini, G., Locatelli, C., Verga, D., 1999. Biotic changes in Cretaceous oceanic anoxic events of the Tethys. *Journal of Foraminiferal Research* 29, 352–370.
- Reboullet, S., Giraud, F., Proux, O., 2005. Ammonoid abundance variations related to changes in trophic conditions across the oceanic anoxic event 1d (Latest Albian, SE France). *Palaios* 20, 121–141.
- Reboullet, S., Mattioli, E., Pittet, B., Baudin, F., Olivero, D., Proux, O., 2003. Ammonoid and nannoplankton abundance in Valanginian (early Cretaceous) limestone-marl successions from the southeast France Basin: carbonate dilution or productivity? *Palaeogeography Palaeoclimatology Palaeoecology* 201, 113–139.
- Roth, P.H., 1978. Cretaceous nannoplankton biostratigraphy and oceanography of the northwestern Atlantic Ocean. In: Benson, W.E., Sheridan, R.E. (Eds.), *Initial Reports of the Deep Sea Drilling Project 44*. U.S. Government Printing Office, Washington, pp. 731–760.
- Savostin, L.A., Sibuet, J., Zonenshain, L.P., Le Pichon, X., Roulet, M.J., 1986. Kinematic evolution of the Tethys belt from the Atlantic Ocean to Pamirs since the Triassic. *Tectonophysics* 123, 1–35.
- Schlanger, S.O., Jenkyns, H.C., 1976. Cretaceous oceanic anoxic events: causes and consequences. *Geologie en Mijnbouw* 55, 179–184.
- Scholle, P.A., Arthur, M.A., 1980. Carbon Isotope Fluctuations in Cretaceous Pelagic Limestones: Potential Stratigraphic and Petroleum Exploration Tool. *The American Association of Petroleum Geologists Bulletin* 64, 67–87.
- Schulze, F., Marzouk, A.M., Bassiouni, M.A.A., Kuss, J., 2004. The late Albian-Turonian carbonate platform succession of west-central Jordan: Stratigraphy and crises. *Cretaceous Research* 25, 709–737.
- Shipboard Scientific Party, 2000. Leg 183 Summary: Kerguelen Plateau-Broken Ridge-A large igneous province. In: Coffin, M.F., Frey, F.A., Wallace, P.J., et al. (Eds.), *Proceedings of the Ocean Drilling Program, Initial Reports 183*, College Station, TX, pp. 1–101.
- Sinton, C.W., Duncan, R.A., 1997. Potential links between ocean plateau volcanism and global ocean anoxia at the Cenomanian-Turonian boundary. *Economic Geology* 92, 836–842.
- Sissingh, W., 1977. Biostratigraphy of Cretaceous calcareous nannoplankton. *Geologie en Mijnbouw* 56, 37–65.
- Snow, L.J., Duncan, R.A., Bralower, T.J., 2005. Trace element abundances in the Rock Canyon Anticline, Pueblo, Colorado, marine sedimentary section and their relationship to Caribbean plateau construction and oxygen anoxic event 2. *Paleoceanography* 20, doi:10.1029/2004PA001093.
- Takahashi, R., Nishi, R., Hayashi, K., Okada, H., Kawahata, H., Yamanaka, T., Fernando, A.G., Mampuku, M., 2009. Litho-, bio- and chemostratigraphy across the Cenomanian/Turonian boundary (OAE 2) in the Vocontian Basin of southeastern France. *Palaeogeography Palaeoclimatology Palaeoecology* 273, 61–74.
- Thomel, G., 1991. Biostratigraphie et faunes d'ammonites du passage Céno-manien-Turonien dans le Sud-Est de la France. Les événements de la Limite Céno-manien-Turonien dans le Domaine Subalpin Meridional et en Provence, Grenoble, 24–26 mai. *Livret-guide*, 57–69.
- Tsikos, H., Jenkyns, H.C., Walsworth-Bell, B., Petrizzo, M.R., Erba, E., Premoli Silva, I., Forster, A., Kolonik, S., Wagner, T., Sinninghe Damste, J.S., 2004. Carbon isotope stratigraphy recorded by the Cenomanian/Turonian Oceanic Anoxic Event: Correlation and implications based on three key-localities. *Journal of the Geological Society, London* 161, 711–719.
- Varol, O., 1992. Taxonomic revision of the Polycyclolithaceae and its contribution to Cretaceous biostratigraphy. *Newsletters on Stratigraphy* 27, 93–127.
- Voigt, S., Erbacher, J., Mutterlose, J., Weiss, W., Westerhold, T., Wiese, F., Wilmsen, M., Wonik, T., 2008. The Cenomanian-Turonian of the Wunstorf – (North Germany): global stratigraphic reference section and new orbital time scale for Oceanic Anoxic Event 2. *Newsletters on Stratigraphy* 43, 65–89.

- Watkins, D.K., 1985. Biostratigraphy and paleoecology of calcareous nanofossils in the Greenhorn Marine Cycle. In: Pratt, L.M., Kauffman, E.G., Zelt, F.B. (Eds.), *Fine-grained deposits and biofacies of the Cretaceous Western Interior Seaway: Evidence of cyclic sedimentary processes*, 4. Society of Economic Paleontologists and Mineralogists, Field Trip Guidebook, Tulsa, pp. 151–156.
- Wilpshaar, M., Leereveld, H., 1994. Palaeoenvironmental change in the Early Cretaceous Vocontian Basin (SE-France) reflected by dinoflagellate cysts. *Review of Palaeobotany and Palynology* 84, 121–128.
- Wilpshaar, M., Leereveld, H., Visscher, H., 1997. Early Cretaceous sedimentary and tectonic development of the Dauphinois Basin (SE France). *Cretaceous Research* 18, 457–468.